| | |
|---|---|
| Band structure of graphene, (a) Full baud structure. (b) Iligh symmetry points of the | Cấu trúc vùng năng lượng của graphene, (a) Cấu trúc vùng năng lượng đầy đủ. (b) |

| | |
|---|---|
| hexagonal Brillouin zone. (The lattice structure is shown in Fig. 8.2**1) (<_) An optical transition near the K point, which corresponds to the circled region of (a). Shading indicates that the states arc occupied. The data in (a) are from Macliou el al. (2002), (c) American Physical Society, reprinted with permission. | Các điểm có tính đối xứng cao của vùng Brillouin lục giác. (Cấu trúc mạng tinh thể được biểu diễn trong Hình 8.2 ** 1) (<_) Dịch chuyển quang học gần điểm K, tương ứng với vùng khoanh tròn trong (a). Vùng mờ ứng với các trạng thái bị chiếm. Dữ liệu trong (a) lấy từ công trình của Macliou và các cộng sự (2002), (c) Đã được Hiệp hội Vật lý Hoa Kỳ cho phép sao chép. |
| 8.5.2 Graphene | 8.5.2 Graphene |
| Graphene is a two-dimensional material with many interesting physical properties. Its band structure is shown in Fig. 8.21(a), with the notation for the high symmetry points of the Brillouin zone given in Fig. 8.21(b).<br>The top of the valence band occurs at the K point, where there is no energy gap to the 7r* states in the conduction band. Figure 8.21(c) shows an enlargement of the band structure near the K point. Note that the bands are linear at this point. | Graphene là một vật liệu hai chiều có nhiều tính chất vật lý thú vị. Cấu trúc vùng năng lượng của nó được biểu diễn trong H. 8.21(a), và kí hiệu các điểm đối xứng cao của vùng Brillouin được biểu diễn trong H. 8.21(b).<br>Đỉnh vùng hóa trị xuất hiện tại điểm K, ở đây chúng ta thấy không có vùng cấm của các trạng thái….trong vùng dẫn. Hình 8.21(c) là ảnh phóng đại cấu trúc vùng gần điểm K. Chúng ta thấy các đường cong tán sắc là các đường thẳng tại điểm này. |
| The linear band dispersion of graphene at the K point gives rise to many striking properties. The most obvious one is tViat all the conduction electrons have the same velocity of ~ c/300, irrespective of their energy. (See eqn 2.25.) This contrasts with the usual behaviour in which E (x k1, and the velocity increases as E increases. The exception to this is when the particle has a negligibly small rest mass. This can be seen from the Einstein energy:<br>Ez = mV + r'V , (8-13)<br>where in is the rest mass micl p is the | Cấu trúc vùng gồm các đường cong tán sắc thẳng của graphene tại điểm K làm nảy sinh nhiều tính chất nổi bật. Tính chất dễ thấy nhất là tất cả các electron dẫn đều có cùng vận tốc ~ c/300, bất kể năng lượng của chúng (xem phương trình 2.25). Điều này trái ngược với tính chất thông thường đó là ….., và vận tốc tăng khi E tăng. Ngoại trừ trường hợp hạt có khối lượng nghỉ không đáng kể. Chúng ta có thể thấy được điều này từ năng lượng Einstein:<br>[redacted] |

linear momentum. The second term dominates when m is negligible, and the energy is linear in p. implying E (x k. The linear dispersion therefore implies that the conduction electrons behave like relativistic particles with negligible mass, and must therefore be treated by the Dirac equation of relativistic quantum mechanics. For this reason, the K point of the Brillouin zone of graphene is known as the Dirac point.

The relativistic properties of the electrons in graphene have many fascinating implications. Here, we concentrate just on the optical properties. These are governed by optical transitions between the valence and conduction bands at the Dirac point, as shown in Fig. 8.21(c). Sincc the energy gap is zero, transitions are possible for all photon frequencies. In a conventional two-dimensional material, the transition rate is imU-pondent, of frequency on account of the constant density of states. 1 6 Section 6.4.2.) This argument., which is based on a parabolic E-k t ispeision, clearly does not apply to graphene. Nevertheless, graphene c oes .show similar behaviour, with the absorption being independent ot the energy at optical frcqucncics. The interesting aspect is that the absorption rate is governed only by the fine structure constant a = e2/ c, with the absorbance ot a single layer being equal to no = 2.3%. We thus have a simple solid state material that clearly illustrates quantum electrodynamical effects.

These predictions for graphene have been confirmed by experiment. Figure 8.22(a) shows the transmission spectrum of a

single1 layer of graphene in the visible spectral region. The data show that the absorbance is indeed independent of the frequency, and takes a constant value of tm = 2.3% per graphene layer. This implies that the transmission of a multilayer sample will be equal to 1 -- naN. where Ar is the number of graphene layers, which is clearly demonstrated by the data for multiple layers shown in Fig. 8.22(b). The absorbance of 2.3% per layer might seem small at first thinking, but is in fact very strong, given that the graphene layer is only one atom thick.

8.5.3 Carbon nanotubes

A carbon nanotube can be considered as a rollcd-up sheet of graphene. There are many different ways to do this, and there are therefore a great variety of nanotube structures. Consider the graphene honeycomb lattice1 shown in Fig. 8.23. The fundamental lattice vectors a\ and a2 of the structure are shown. In a nanotube. the1 graphene sheet is rolled up so that one of the translation vectors e)f the1 la11 ice1 becomes the circumference. We can thus define the circumference vector of the nanotube a.s:

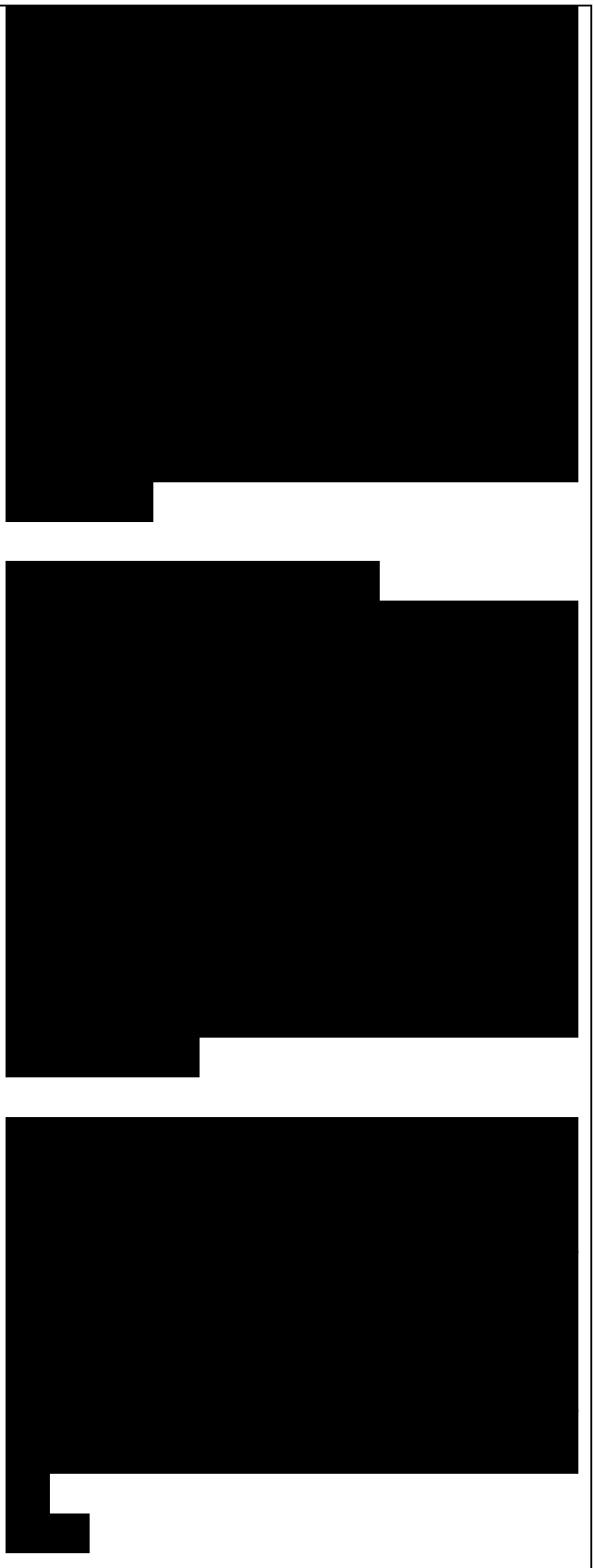

Fig. 8.22 (a) Transmission of a single' layer of graphene in the visible spectral region. The dashed line is the transmission expected tor a constant absorbance of 7tq. The slight drop in the transmission at short wavelengths is possiblv caused by hydrocarbon contamination (b) Variation of the transmission with the number of graphene layers. Alter Nair et al. (2008), © AAAS, reprinted with permission.

(8.14)

where n\ and 112 are integers, and the tube axis is perpendicular to c. This circumfcrcnec vcctor is usually called the chiral vector and is denoted (??i.n2). The diameter of a nanotube is given by (see Exercise 8.18):

ai\ = \a2\ = 0.2461 nm is the length of the basis vectors.

Three different, types of circumference vectors are indicated in Fig. 8.23. TIio.se with 112 = 0 and n-z — ni called 'zigzag' and ‘armchair nanotubes respectively, and all the remainder are simply called 'chiral . The chiral angle H is defined as the angle between the chiral vector and the zigzag direction, and is given by (sec Exercise 8.18):

Armchair mmotubcs 11ms have chiral angles ol 30°.

Fig. 8.23 Definition of the lattice vectors ai and a.2 for the graphene lattice, and the chiral vectors for a nanotube. The chiral angle 0 is the angle between the chiral vector and the 'zigzag' direction.

In discussing the properties of carbon nanotubes, it is important to distinguish between single-walled nanotube (SYVNT) and multi-wall nanotube (MWNT) structures. As the names suggest, these correspond respectively to nanotubcs composed of a single cylinder with a unique chiral vector, and those composed of several concentric cylinders with differing chiral vectors. Much progress has been made in recent years in techniques to isolate individual SWNTs, making the study of nano tubes with well-defined chiral vectors possible.

The electronic properties of nanotubes follow from their chiral structure. We have seen that graphene is a semimetal on account of its zero energy gap at the K point of the Brillouin zone. (See Fig. 8.21.) Nanotubes, by contrast, can be either metallic or semiconducting. The nanotube is metallic if (see Exercise 8.19):

[redacted]

Multi-wall nanotubes will typically contain some metallic and some semiconducting tubes, and will therefore usually be highly conducting.

[redacted]

where m is an integer (positive, negative, or zero). In all other cases the nanotube is a semiconductor with a finite energy gap between the conduction and valcncc bands. It is therefore apparent that one-third of nanotubes are metallic, and two thirds semiconducting.

The electrons in a nanotube are free to move along the axis (usually defined as the 2 direction), but experience two-dimensional cylindrical confinement in the perpendicular directions. We thus have an almost ideal one-dimensional system, which can be treated as a quantum wire. (See Section G.l.) The wave functions of the electrons are of the form:

[redacted]

where kz is the wave vector along the tube axis, L is the normalization length, and (i, j) arc indices that identify the quantum-confined circum-ferential states of the tube. The energy of the electrons is therefore given by:

[redacted]

where n is an integer that, specifies the quant uui-eonfiiiod density of states per unit, length for each band is given Incise 8.20):

[redacted]

as appropriate for a 1-D material. We thus expect, van Hove singularities in the density of states at the energies of each quantized level.

Figure 8.24 illustrates the band structure for semiconducting and metallic nanotubes together with their density of states. For each confined state we have a parabolic band, with a van Hove singularity at the energy threshold. In semiconducting nanotubes, there is an energy gap between the highest filled state in the valence band and the lowest empty slate in the conduction band, a.s shown in part (a). The magnitude of this gap varies with the tube diameter and lies at about 0.8 eV (1500nm) for a tube with a diameter of 1 mn. (Sec Fig. 8.25.) Metallic nanotubes have the additional linear band derived from the K point of the Brillouin zone of graphene. (See Fig. S.21 and its discussion.) Sincc the band passes through the origin, I here is no gap between the top of the valence band and the bottom of the conduct ion baud. There is therefore a continuum of states between the quantum-confined levels, as .shown in part (b) of’Fig. 8.24.

Optical transitions can occur between states in the valence band and the conduction band. 7’hc selection rules dictate that the quantum number n 'if the electron and hole states must be identical, and conservation uf momentum requires ihaf /c- is unchanged. Owing to the van Hove sin-

See Scction 3.5 for an explanation of van Hove singularities.

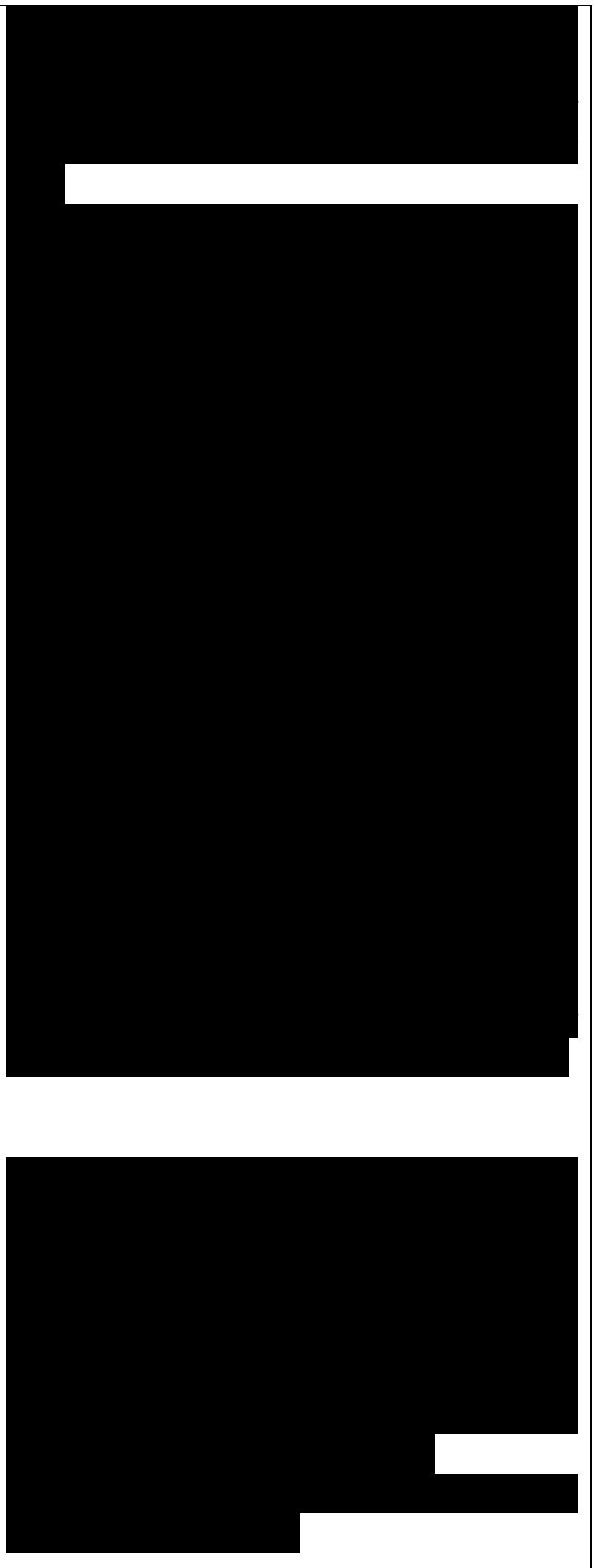

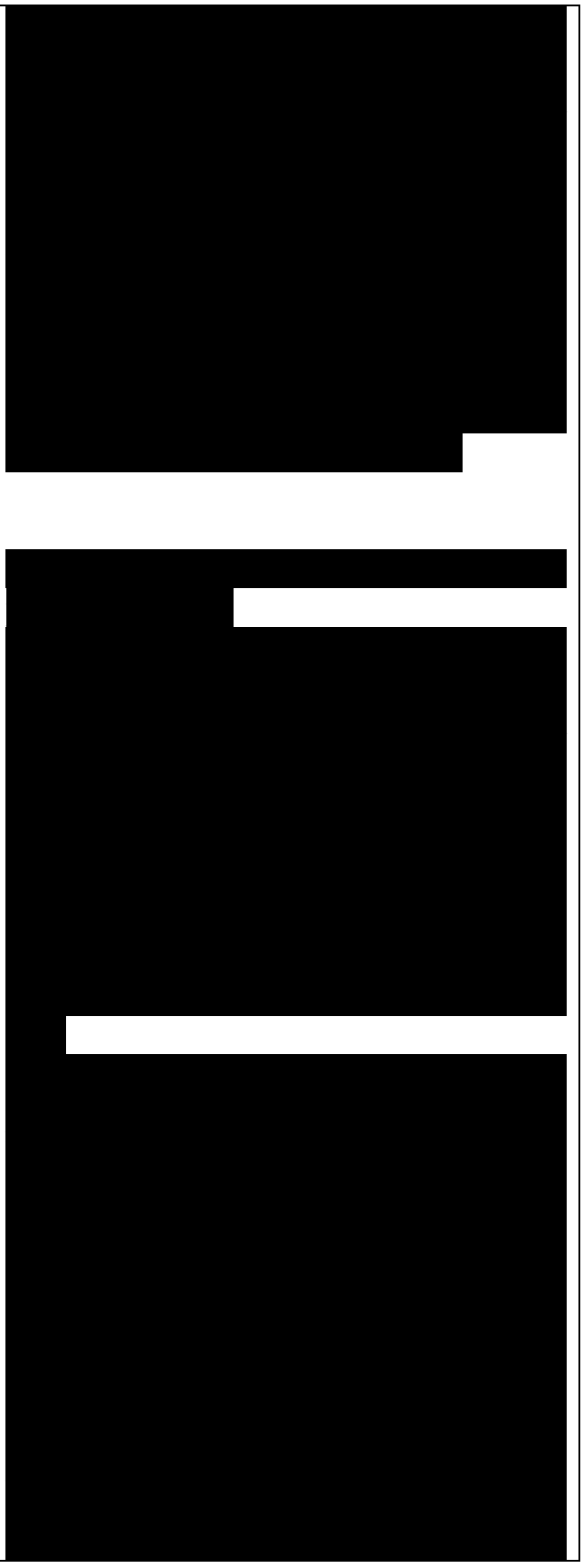

Fig. 8.25 Kataura plot of the calculated energies of the confined states versus tube diameter. The solid and open circles correspond to semiconducting and metallic nanotubes respectively. The first three energy states are labelled according to the notation of cqti 8.21, with additional superscripts to identify semiconducting (s) and metallic (m) nanotubes. See Kataura et al. (1999). Data from Dr S. Maruyama, www.photon.t.u-tokyo.
ac.jp/~mRruyama/iianotube.html.

gularities at the threshold for each band, the transition late at photon energies that satisfy

where the superscripts identify the conduction and valence, bauds re spectively. The En and £22 transitions are illustrated for both semiconducting and metallic nanotubcs in Figs 8.24(a) and (b) respectively. Optical transitions are, of course, possible at other photon energies, but the transitions at the frequencies that satisfy eqn 8.21 are expected to stand out from the continuum 011 account of their higher transition rate.

Fluorescence can be observed in semiconducting nanotubcs when electrons excited in the conduction band recombine with holes in the valence band. This is typically done by exciting electrons and holes into a higher band by photo-excitation. The electrons and holes then relax by plionon emission to the lowest bands, and emit photons with energies given by u> = En. This process is illustrated in Fig. 8.24(a) for the case where the electrons and holes are initially excited in the n — 2 bands. Fluorescence

is not observed from metallic nanotubes because the hole in the valence band is very rapidly refilled by electrons from the occupied states above it..

Figure 8.25 shows a plot of the energy gap defined by eqn 8.21 as a function of the tube diameter. Such a diagram is called a ‘Kataura’ plot. The solid and open circles coiTcspond to semiconducting and metallic nanotubes respectively. As we would expect for a quantum confinement effect, the magnitude of the energy gaps decrease as the tube diameter increases, varying roughly as 1/e/. For any particular tube, there is a series of energy gaps that correspond to increasing values of 11. The fundamental band gap (/vj1,) of the semiconducting tubes moves into the visible spectral region for tube diameters smaller than about 5nm. Note that the zero gap states of the metallic tubes are not shown in

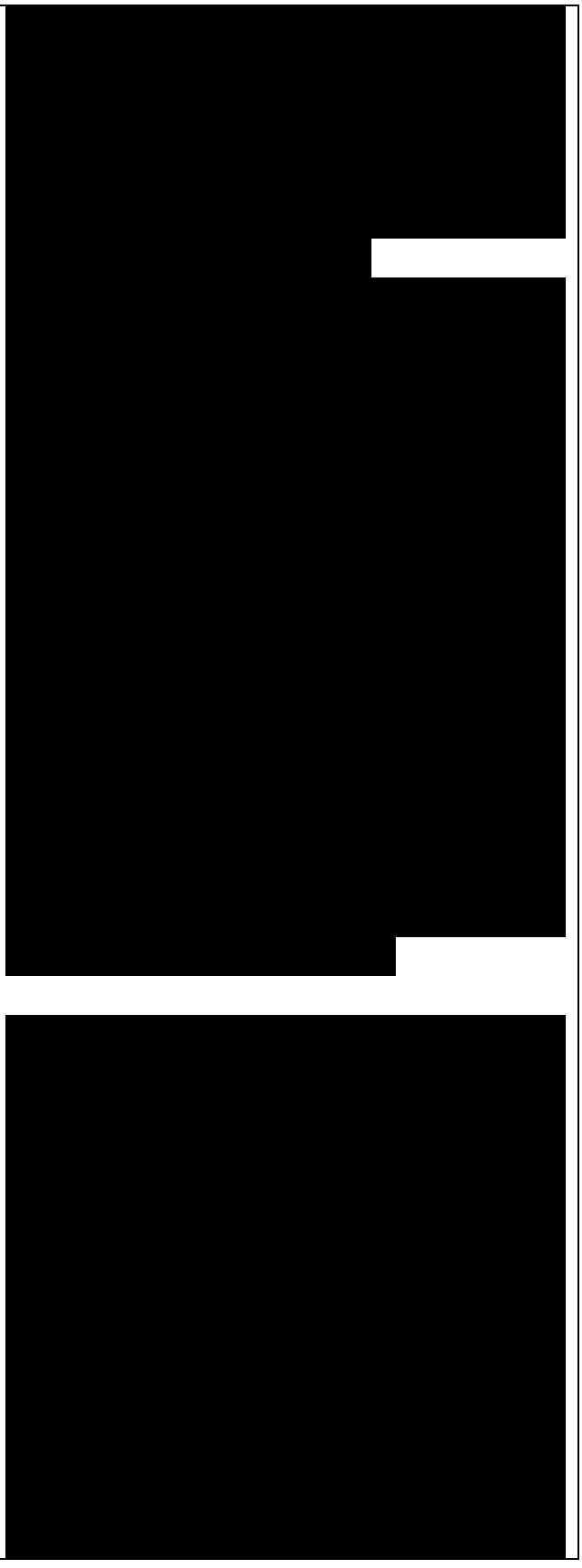

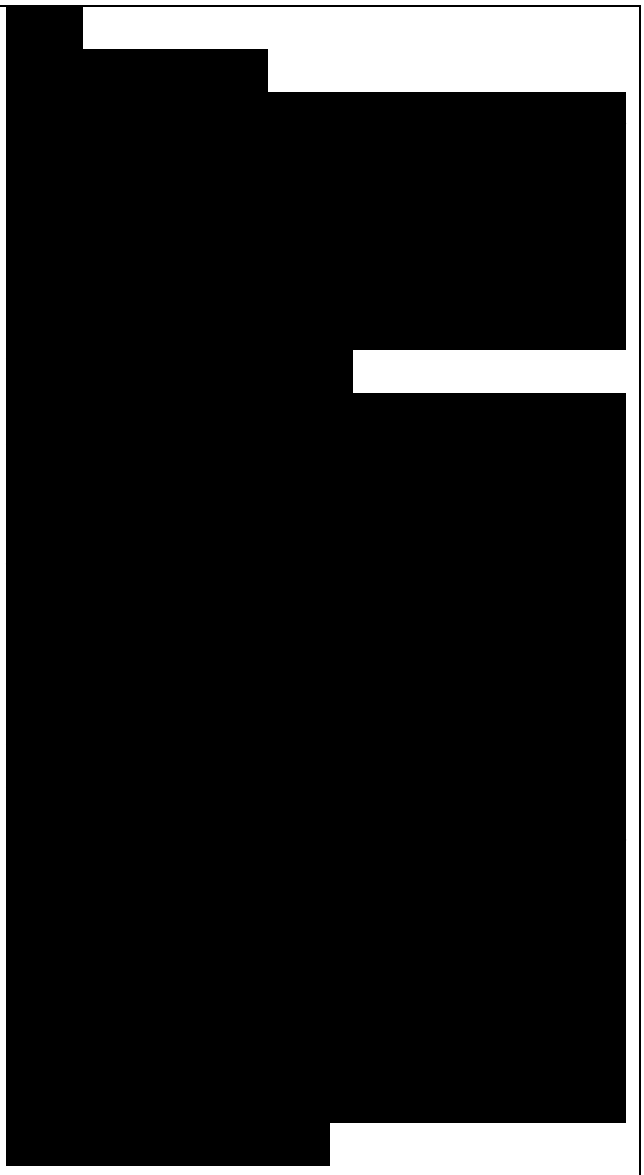

The discussion above makes no consideration of excitonic effects. The exciion binding energy Ex in a carbon nanotube is much larger than in a typical bulk III V semiconductor due to its reduced dimensionality. The binding energy varies inversely with the diameter, and is given roughly Uv E\ ~ 0.3/d when E\ is measured in eV and d in 11111. This implies that E\ 0.1 eV for <7 = 0.811111. As explained in Chapter 1, tlie dominant excitonic transition occurs at (EQ; — E\).

where £V; is the band gap and Ex is the cxcitun binding energy. This implies that the actual band gaps arc somewhat

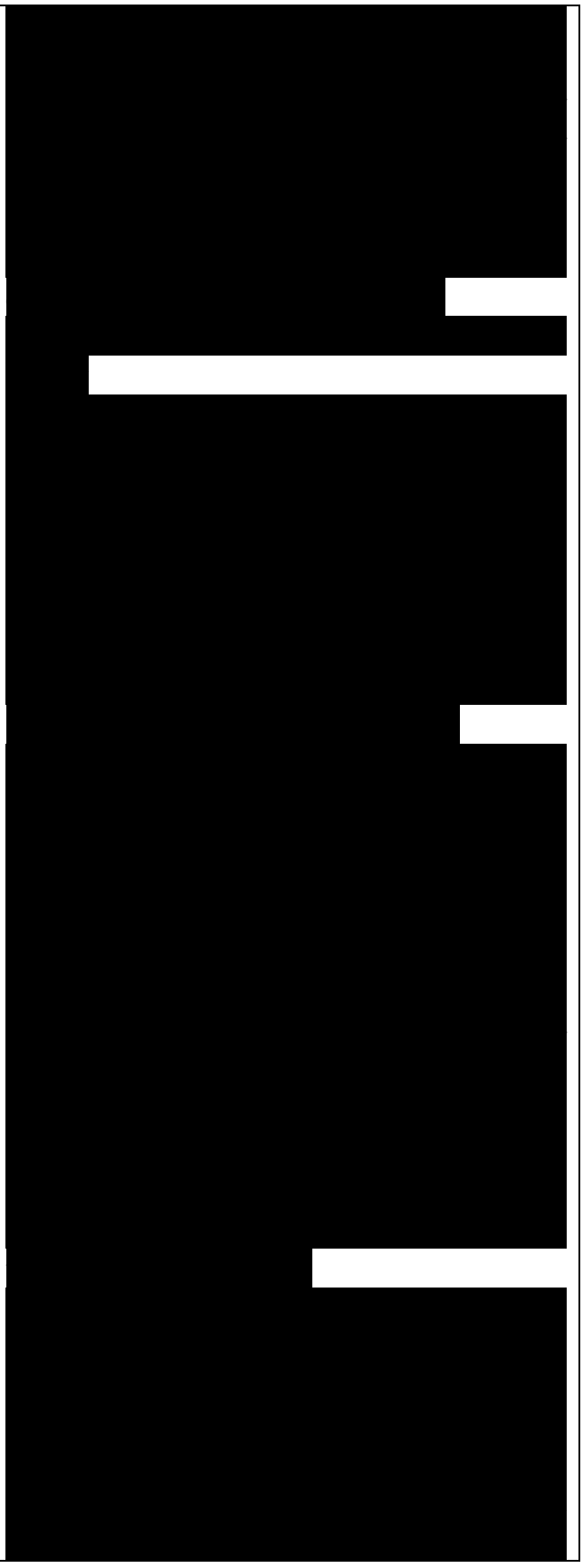

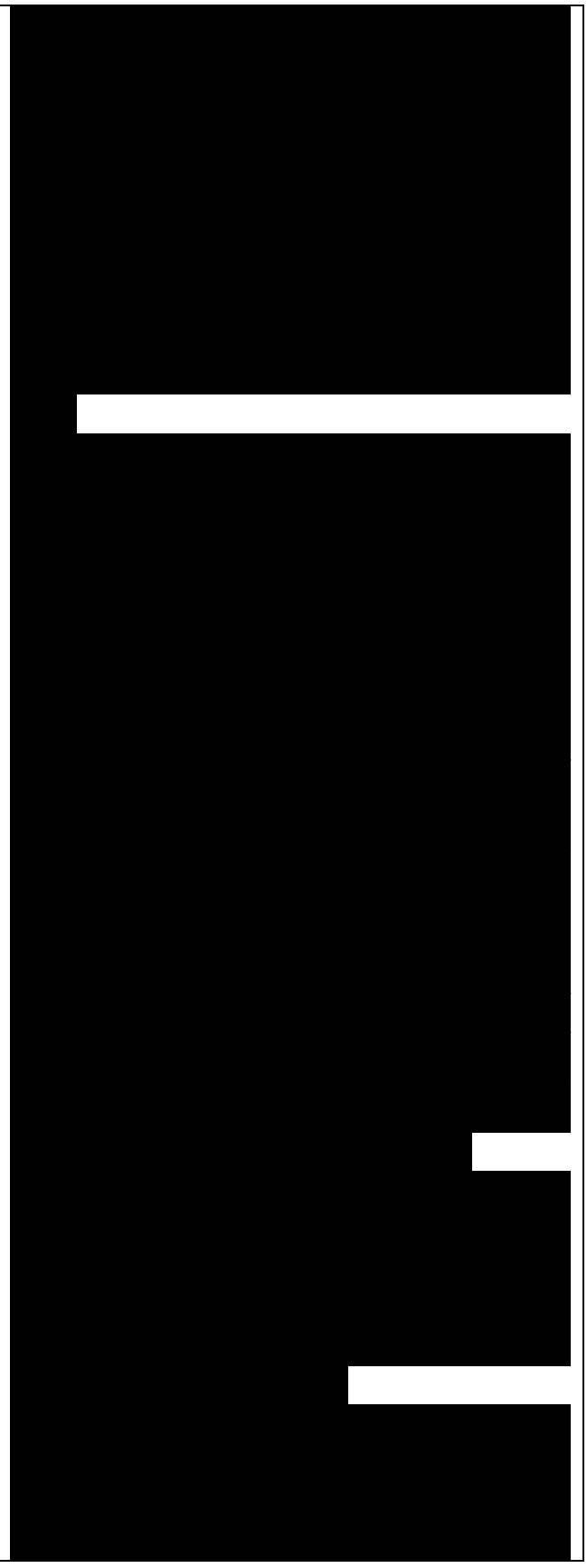

Fig. 8.27 (a) Jablonski diagram lor C(>(). The* labels g* and ’if denote the parity of the states. The solid arrows indicate optical transitions, while the dashed arrows indicate noil-radiative relaxatfon processes. The time constants) indicated art* typical values and can vary somewhat from sample to sample, (b) Absorption spectrum of z\. C\>o thin film at room teinperatuie. I he inset shows the absorption and normalized photolumiriescence (PL) (dotted line) spectra for crystalline Coo at- 10K. 1 lie grey and black arrows indicate the onsets of the So —* Si and So —* S2 transitions, respectively. Data taken (rom Ren et al. (1991). © American Institute of Physics, and Schlaich et al. (1995), © Elsevier, reprinted with permission.

Note that the time constants quoted here are only typical values, and can vary significantly between samples. The intersystem crossing rate in Cco is rela- tively fast because the Si and Tj levels are nearly degenerate.

This long radiative lifetime has to be compared to the shorter inter- system crossing time of 1.2 ns. The T t —> So transitions arc strongly forbidden and

hence have a very low probability, effectively making the decay route via Tj a non-radiative channel. It is therefore apparent from eqn 5.5 that the radiative efficiency is very low, with typical values being around 10“3 for crystalline Coo at low temperatures.

Figure 8.27(b) shows the absorption spectrum of a solid C’oo thin film at room temperature. The absorption at the HOMO —* LUMO gap of 1.85 eV is weak, as expected for dipole-forbidden transitions, and the first strong feature is observed at 2.7 cV. which corresponds to the So —» S2 transition. The strong line at 3.6 eV corresponds to a transition from an odd parity lower level in the valence band to the even parity S\ level, while the line at 4.7eV arises from So —* Sfl transitions, where S,, is the next odd parity singlet excited state above S2.

The inset in Fig. 8.27 shows the photolmnincscenec (PL) spectrum of crystalline C’oo 10 K and the detailed absorption spectrum at the HOMO-LUMO band gap. As mentioned above, electric-dipole transitions between the HOMO and LUMO states are forbidden by the parity .selection rule. This means that the transitions must occur either by higher-order processes (e.g. electric quadrupole) or by a mechanism that destroys the parity of the states. Examples of the second type of mechanism include crystal disorder and vibronic coupling. These both lead to distortions of the icosahedral symmetry of the Coo molecule—static in the former case and dynamic in the latter—and hence to a loss

of the ^ 5 ion symmetry that, defines the parity.

Both the absorption and PL spectra in the inset of Fig. 8.27 exhibit stlong vibionic sub-structure, together with additional peaks caused by t le fine structure of the Sj level. The relative intensity of the vibronic peaks in the PL spectrum is found to vary significantly from sample to sample on account of the strong sensitivity to defects and crystalline disorder. The purely electronic 0-0 vibronic line occurs at 1.84fieV and is identified by the grey arrow. The fact that this line is absent from the PL spectrum clearly demonstrates that vibronic coupling (i.e. coupling to plionmis) is an important factor in allowing the radiative emission lo occur.

Carbon bucky balls have potential applications as optical limiting de-vices in the spectral region 500-800 nm. The absorption rate is small at low powers, since the photon energy lies below the So —> S2 threshold at 2.7 cV. As the power is increased, the photo-excited electrons transfer rapidly to the lowest triplet state by intersystem crossing and accumulate there 011 account of the long lifetime of the Ti level. These electrons can then absorb light in the same spectral region by making transitions to odd parity triplet excited states. A new absorption channel thus opens up at high intensities, which thereby limits the transmission of high power pulses. Such an optical limiter is potentially useful for making safety goggles to protect the eye from intense laser pulses.

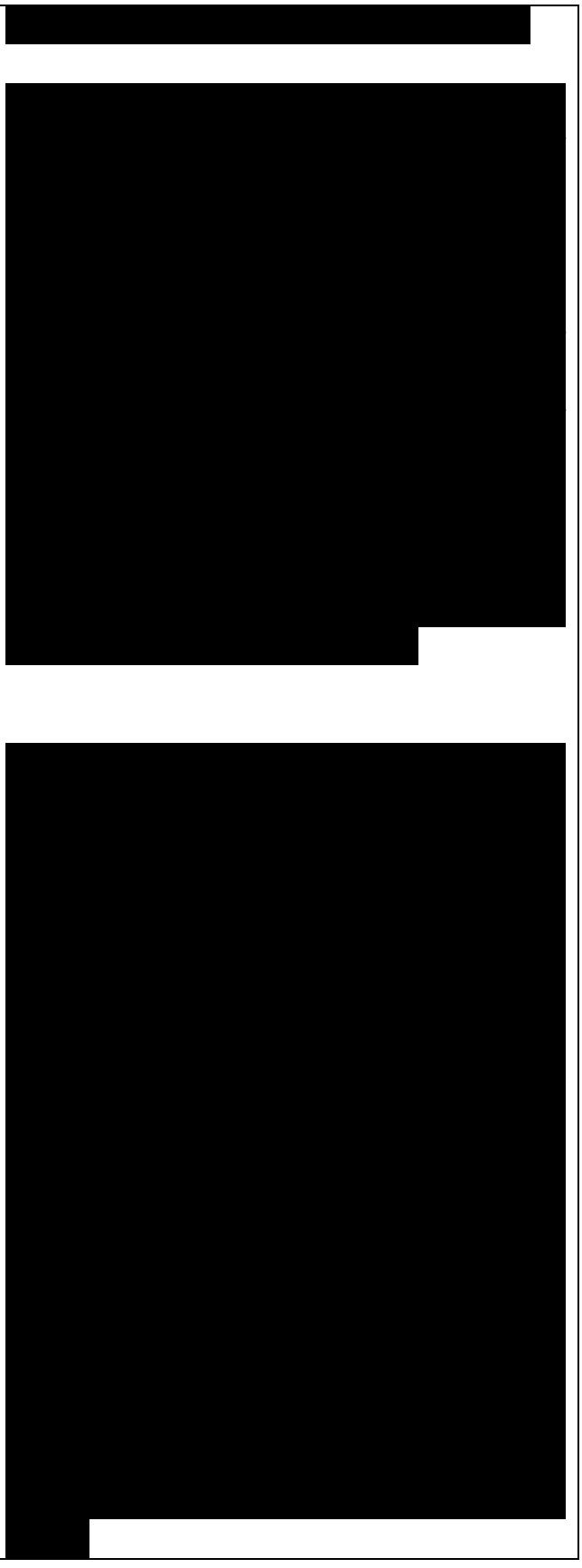

| | |
|---|---|
| The lifetime of the T1 level is very long (> 50 ms) because the transitions to the So level violate both the spin and parity selection rules. | [redacted] |